

## Tomographic estimation of compressional and shear wave velocities from *P-S* converted waves

Claudio D'Agosto and Reinaldo J. Michelena\*, Intevep, S.A.

### Summary

We present a tomographic method to estimate simultaneously *P*- and *S*- wave velocities in horizontally, layered media from traveltimes of reflected, *P-S* converted waves. The method is based on the exact expression for the traveltimes of *P-S* converted waves in layered media. This expression is valid for any offset since the position of the conversion point is calculated analytically without any approximation. The largest singular value of the Jacobian matrix that results after linearizing the traveltime function are related to variations in shear wave velocities whereas the smallest singular values are related to variations in layer thickness. Therefore, when inverting the linearized problem by using conjugate gradients, shear wave velocities converge faster than compressional wave velocities. Layer thicknesses are the hardest to obtain. Singular values related to shallow layers are larger than singular values related to deep layers which means, as expected, parameters that describe shallow layers are easier to obtain than parameters of deep layers. Our synthetic examples show that by starting the iterative procedure with initial models whose *P*-wave velocities are close to the true model, it is possible to retrieve almost exactly compressional velocities, shear velocities, and layer thicknesses. When the initial model for *P*-wave velocities is not as good, it is still possible to obtain useful results.

### Introduction

The use of *P-S* converted waves has increased over the last few years after various studies have demonstrated their tremendous potential as a tool for fracture and lithology characterization (Ata and Michelena, 1995; Miller et al., 1995), imaging sediments in gas saturated rocks (Granli et al., 1995), and imaging shallow sediments with higher resolution than conventional *P-P* data. The reasons for the increased use of *P-S* converted waves over *S-S* surveys are two fold: converted waves cost less and are expected to contain the same information, in principle, as *S-S* reflections. However, even though *P-S* converted waves are less affected by azimuthal anisotropy than nonconverted *S-S* waves, the asymmetry of the ray paths for converted waves makes them more cumbersome to handle than nonconverted waves and more difficult to process to extract information about *S*-wave velocities.

When the  $v_p/v_s$  ratio is needed for converted waves processing (for common conversion point gathering) or interpretation (for lithology estimation), it is always estimated from the ratio of traveltimes  $t_s/t_p$  by assuming that the vertical distance traveled by the *P*- and *S*-rays is the same. However, in cases when the *S*-wave velocity is needed for other purposes than computing the  $v_p/v_s$

ratio (for instance, pre-stack depth migration of converted waves), its estimation from converted, reflected arrivals is more difficult because conventional velocity analysis techniques of converted waves gathers only yields a velocity that is somewhere in between *P*- and *S*-wave velocity.

Few work has been done in the development of methods to estimate  $v_s$  from converted waves. Stewart (1991) and Ferguson and Stewart (1995), show a method to estimate *S*-wave velocities from the reflectivity of *P-S* data. However, as far as we know, no method has been developed yet to estimate *P*- and *S*-velocity models in depth from converted waves energy. This paper presents a tomographic technique to solve such a problem for horizontally layered media. Tomographic estimation of velocities is not an efficient method of velocity estimation in layered media from nonconverted reflections. However, as we show in this paper, traveltime tomography is a valid alternative for converted, reflected waves since conventional velocity analysis of these data does not yield *S*-wave velocities.

We start by developing the analytical expression for the traveltime of a *P-S* converted wave that travels in a homogeneous, isotropic layer. After generalizing this expression to stratified media, we study the singular values of the Jacobian matrix that results after linearizing the analytical traveltime function. The algorithm estimates simultaneously compressional velocities, shear velocities and layer thicknesses of stratified models. The analysis of both singular values of the Jacobian matrix and synthetic examples show that when the problem is solved iteratively, the speed of convergency of the different parameters varies, being *S*-wave velocities the fastest and layer thicknesses the slowest. Synthetic examples also show that excellent estimates of compressional and shear velocities in depth can be obtained if the initial model for *P*-waves velocities is close to the true solution.

### Traveltime for *P-S* converted waves in layered media

Consider a reflected, converted wave over an horizontal interface located at a depth  $h$  [Fig. (1)]. The conversion point CP is closer to the receiver position since, according to Fermat principle, for the traveltime between sources and receivers to be the smallest, the portion of the ray that travels with *P* wave velocity should be larger than the portion of the ray that travels with *S*-wave velocity.

The traveltime for a ray that travels from  $s$  to  $g$  (Fig. 1) is simply the sum of the times it takes to travel to the interface with *P*-wave velocity ( $t_p$ ) plus the time it takes to go up again to the geophone with *S*-wave velocity ( $t_s$ ):

$$t = t_p + t_s, \quad (1)$$

or

$$t = \frac{\sqrt{(r-x)^2 + h^2}}{v_p} + \frac{\sqrt{x^2 + h^2}}{v_s}. \quad (2)$$

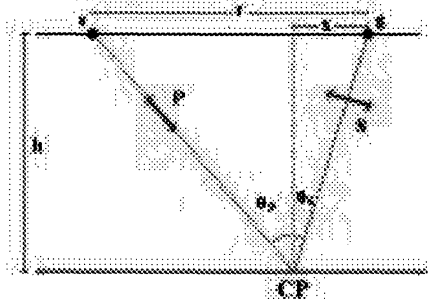


FIG. 1. P-S reflection over an horizontal interface, in an homogeneous and isotropic media.

where  $x > 0$  is the position of the conversion point measured from the receiver position. After introducing Snell's law in equation (2) we get a fourth order polynomial in  $x$

$$x^4 - 2rx^3 + (r^2 + h^2)x^2 - \frac{2rh^2}{K}x + \frac{r^2h^2}{K} = 0, \quad (3)$$

where:

$$K = 1 - \frac{v_p^2}{v_s^2} < 0. \quad (4)$$

Equation (3) has four roots, but only one of them yields  $x > 0$  for  $K < 0$ . The analytic form of these roots was calculated using Maple( TM).

Fig. (2) shows the trajectory of the  $j$ th P-ray converted to S at the  $n$ th interface of a horizontally layered medium. The traveltimes of such a ray is a simple generalization of equation (1), as follows:

$$t_j = \sum_{i=1}^{n-1} t_{p_{ji}} + \sum_{i=1}^{n-1} t_{s_{ji}} + t_{jn}, \quad (5)$$

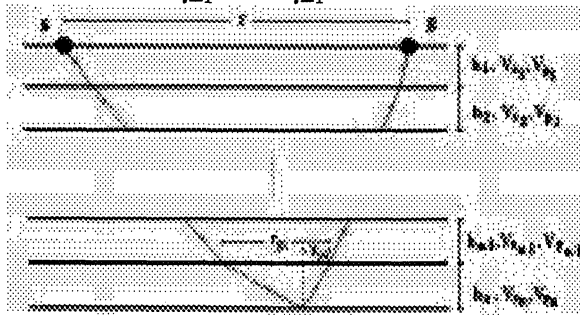


FIG. 2. P-S converted wave traveling in a layered media

where  $t_{p_{ji}}$  is the traveltimes of the  $j$ th, P-wave ray on the  $i$ th layer. The quantity  $t_{s_{ji}}$  has an analogous definition for S-waves. The last term of equation (5) ( $t_{jn}$ ), corresponds to the traveltimes in the layer where the reflection occurs [equation (2)]. If the traveltimes within this particular layer is not explicitly separated from the

other two sums in equation (5) but, instead, each of the two sums is taken up to the  $n$ th layer, the position of the conversion point becomes another unknown of the problem. Equation (5) does not have the conversion point as unknown because such a point has been explicitly calculated by introducing Snell's law. After introducing the distance traveled by the ray within each layer in equation (5), we obtain

$$t_j = \sum_{i=1}^{n-1} \frac{1}{v_{p_i}} \sqrt{(\Delta x_{p_{ji}})^2 + h_i^2} + \sum_{i=n-1}^1 \frac{1}{v_{s_i}} \sqrt{(\Delta x_{s_{ji}})^2 + h_i^2} + \sqrt{(r_{jn} - x_{jn})^2 + h_n^2} \frac{1}{v_{p_n}} + \sqrt{x_{jn}^2 + h_n^2} \frac{1}{v_{s_n}}, \quad (6)$$

where  $v_{p_i}$  and  $v_{s_i}$  are the P- and S-wave velocities, respectively, in the  $i$ th layer.  $\Delta x_{p_{ji}}$  and  $\Delta x_{s_{ji}}$  are the horizontal distance traveled by the P- and S-wave in the  $j$ th ray in the  $i$ th layer.  $r_{jn}$  and  $x_{jn}$  are defined in Fig. (2). This equation is the heart of the inversion procedure proposed in this paper.

#### Parameter estimation

Equation (6) relates nonlinearly the unknown model parameters  $v_{p_i}$ ,  $v_{s_i}$ , and  $h_i$  with the measured traveltimes  $t_j$ . Linearization of equation (6) yields a simpler relation between traveltimes and model parameters:

$$J \Delta \vec{m} = \Delta \vec{t}, \quad (7)$$

where columns of the matrix  $J$  (the Jacobian) are the partial derivatives of the traveltimes function (6) with respect to the model parameters  $\vec{m}$ ,

$$\vec{m} = (h_1, h_2, \dots, h_n, v_{p_1}, v_{p_2}, \dots, v_{p_n}, v_{s_1}, v_{s_2}, \dots, v_{s_n}). \quad (8)$$

$\Delta \vec{t}$  is the vector of differences between measured and calculated traveltimes in each iteration. Point to point ray tracing was performed over the synthetic models to compute traveltimes of converted waves and the distance traveled by the ray in each layer. Equation (7) is solved by LSQR (Paige and Saunders, 1982).

#### SVD analysis of the Jacobian matrix

Singular value decomposition (Golub and Van Loan, 1989) was performed on the Jacobian matrix  $J$  to understand the sensitivity of the different model parameters with respect to the traveltimes. In this particular work, we concentrated our analyses on the variations of the singular vectors that span the model space with respect to the size of their corresponding singular value.

As equation (8) shows, the first third of the vector of model parameters  $\vec{m}$  contains information about variations in layer thicknesses ordered from the shallowest to the deepest layer, the second third contains information about variations in compressional velocities, and the last third contains information about variations in shear

wave velocities. Fig. (3) shows how the singular vectors of  $J$  that span the model space change with respect to the size of the singular value for a simple model of 3 sources and 3 receivers over a 10 layers, linearly increasing velocity model. For this case, the model space has dimension 30.

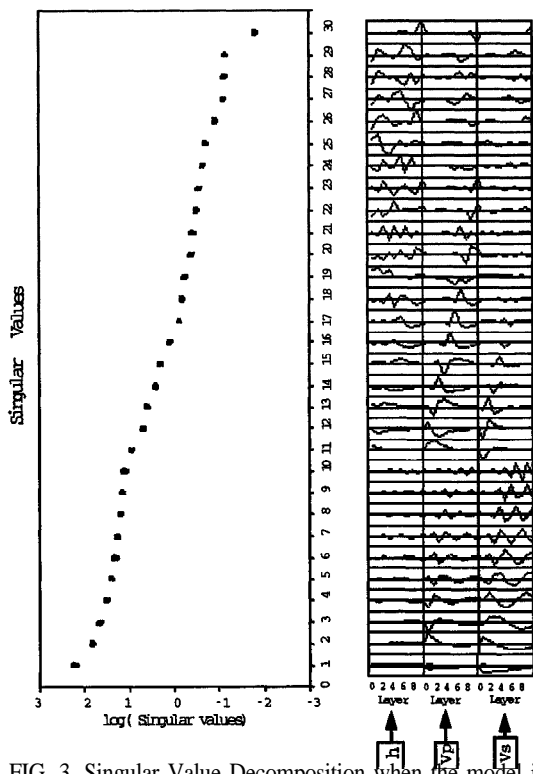


FIG. 3. Singular Value Decomposition when the model is described by 10 horizontal layers and the recording geometry consist of 3 sources and 3 receivers. Left: Logarithm of the singular value. Right: Corresponding singular vectors that span the model space

From Figure (3) we observe the singular vectors related to the first 10 singular values have more variations over the portion that corresponds to S-wave velocity, the following 10 singular vectors contain more variations over the portion that correspond to P-wave velocities, and the last eigenvectors have more variations over the layers thicknesses. On the other hand, the largest singular values are related to singular vectors that contain no information about layer thickness and the smallest ones contain almost no information about shear wave velocities. From these results we can conclude that S-wave velocities will converge faster to the final solution than P-wave velocities if the system of equations (7) is solved by iterative methods such as conjugate gradients. According to Stork (1988), the first iterations of conjugate gradients resolve information contained in singular vectors related to the largest singular values whereas much more iterations are needed to retrieve the information related to the smallest singular values. Layer thicknesses will have the slowest rate of convergency. We can observe this behavior in Fig. (4) that shows how the dif-

ferent parameters converge towards the true solution as a function of the number of iterations for the simple 10 layers, linearly increasing velocity model. After a few iterations, S-wave velocities are closer to the true solution than both P-wave velocities and layer thicknesses.

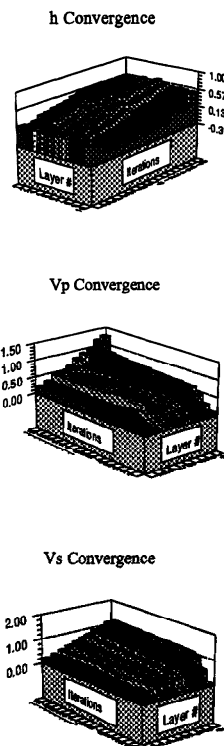


FIG. 4. Parameter convergency

Perturbations in shear wave velocities produce less changes in the ray path than perturbations in both compressional velocities and layer thicknesses, as Fig. (5) shows. Therefore, shear velocities converge faster since ray paths are closer among themselves. On the other hand, for variations in compressional velocities and layer thickness, the difference among ray paths is greater and, as a result, the convergence of these parameters is slower. Unknown ray paths are more stable with respect to changes in shear velocities than with respect to changes in the other parameters.

#### Synthetic examples

We generated synthetic traveltimes for a recording geometry that consists of 100 geophones (15 m apart) and 3 sources (15 m apart also). The minimum offset was 30 m. The model have 10 layers of equal thickness and equal to 500 m. As Fig. (6a) shows, when starting the iterations with an initial model far from the true solution, the algorithm can estimate the model parameters with error less than 10% when compared to the true values. When the initial P-wave velocities and the layer thicknesses are close to the true values, the estimated shear velocities are retrieved almost perfectly, as

Fig. (6b) shows.

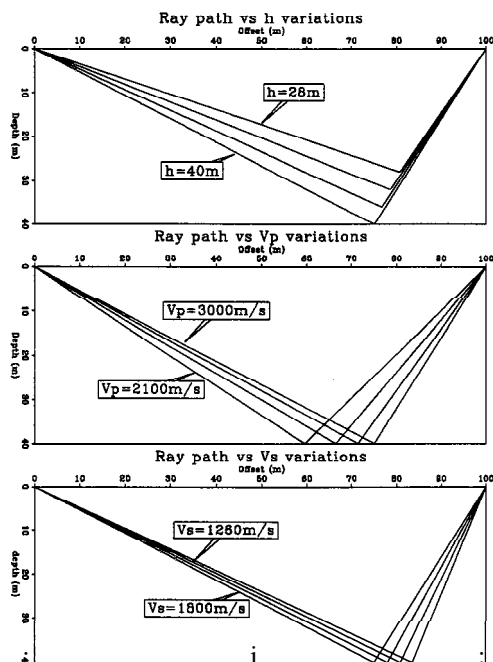


FIG. 5. Ray path behavior related to changes in model parameters

### Conclusions

We have presented a method to estimate tomographically compressional velocities, shear velocities and layer thicknesses from traveltimes of P-S reflected waves. If the initial model for compressional velocities is close to the true solution, shear velocities can be accurately estimated. Additionally, we have seen that the S-wave velocity is the parameter that converges faster to the final solution when compared to the speed of convergence of P-wave velocity and layer thicknesses, which are the slowest to converge. As expected, parameters related to shallow layers converge faster than parameters that describe deep layers. The differences in speed of convergence are explained in terms of the singular values of the Jacobian matrix and the relative changes of unknown ray paths with respect to changes in models parameters. The largest singular values of the problem are related to changes in shear velocities, and these changes have the smallest influence in the ray trajectories when compared to the influence of changes in the other parameters.

### Acknowledgements

The authors would like to express their thanks to INTEVEP, S.A. for permission to publish this research. Thanks to Debora Cores for providing the ray tracing algorithm.

### References

- Ata, E. and Michelena, R. J., 1995, Mapping distribution of fractures in a reservoir with P-S converted waves, *The Leading Edge*, 14, no. 6, 664-673.
- Ferguson, R. and Stewart, R., 1995, Estimating shear-wave velocity from P-S seismic data, 65th Annual Internat. Mtg., Soc. Expl. Geophys. Expanded Abstracts, 95, 1036-1039.

- Golub, G. and van Loan, C., 1989, *Matrix computations*, Johns Hopkins Univ. Press.
- Granli, J.R., Sollid, A., Hilde, E. and Arnsten, B., Imaging through gas-filled sediments with marine S-wave data, 65th Annual Internat. Mtg., Soc. Expl. Geophys., Expanded Abstracts, 95, 352-355.
- Miller, S.L.M., Harrison, M. P., Lawton, D.C., Stewart, R.R. and Szata, K.T., 1995, Coupled P-P and P-SV Seismic Analysis of a Carbonate Reservoir, Alberta, Canada., 57th Mtg. Eur. Assoc. Expl. Geophys., Extended Abstracts, 95, Session:A015.
- Paige, C. and Saunders, A., 1982, LSQR: An algorithm for sparse linear equations and sparse least squares, *ACM Trans. Math. Software*, 8, No. 1, 43-71.
- Stewart, R. R., 1991, Rapid map and inversion of P-SV waves: *Geophysics*, 86, 859-862.
- Stork, 1988, Comparison of Richardson's iteration with Chebyshev acceleration factors to conjugate gradient iteration, *Stanford Expl. Proj. SEP-57*, 479-503.

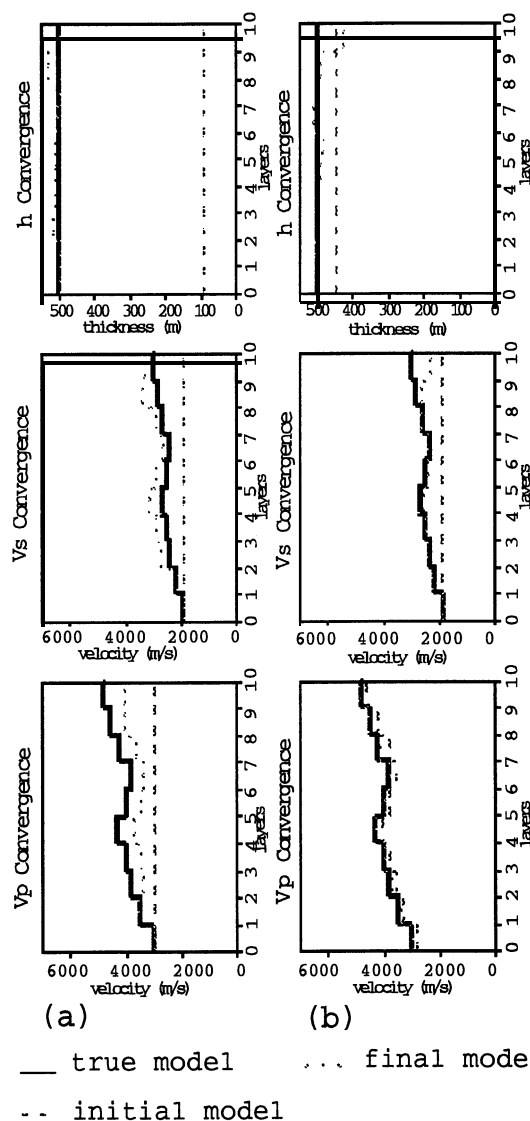


FIG. 6. Result of the inversion for a model described by 10 horizontal layers and the recording geometry consisting of 3 sources and 100 receivers. (a) initial model far from the true solution. (b) initial P-wave velocities and layer thicknesses close to the true values .